

ORIGINAL ARTICLE

Cardiac structural remodeling in hypertensive cardiomyopathy

Si-jia Sun^{1,3}, Jia-lu Yao^{1,2,3}, Lang-biao Xu¹, Qing Rui¹, Nan-nan Zhang¹, Min Chen¹, Yu-feng Jiang¹, Hua-jia Yang¹ and Ya-feng Zhou¹

Heart failure with preserved ejection fraction (HFpEF), which is a primary driver of morbidity and mortality, accounts for approximately half of all heart failure cases. Therefore, it is essential to develop preclinical animal models for HFpEF pharmacological treatment strategies. We created a porcine model of severe hypertension and hyperlipidemia by using a combination of deoxycorticosterone acetate (DOCA, 100 mg kg⁻¹), Western diet (WD) and angiotensin II infusion. Systolic blood pressure, echocardiography and invasive pressure–volume loop were assessed at baseline, 12 weeks and 18 weeks. A detailed histological assessment was also performed to determine the cardiac structural remodeling. Compared with controls ($n=10$), hypertensive animals ($n=10$) showed markedly higher systolic blood pressure (181 vs. 126 mm Hg) at 18 weeks. Concentric remodeling, characterized by a normal chamber size with a thicker wall, was observed in hypertensive animals. Left ventricle diastolic function showed a tendency toward decline, according to the echocardiographic data. Hemodynamic data showed that the end-diastolic pressure–volume relationship was elevated without changes in the end-systolic pressure–volume relationship. Histological results revealed that the fibrotic area in hypertensive animals ($P<0.05$ vs. controls) and the fibrotic area in the posterior wall of hypertensive animals' left atria were larger than other sites of the left atria ($P<0.05$ vs. other sites). This model can mimic clinical HFpEF to some degree. We found that the posterior wall of the left atrium is more susceptible to atrial remodeling associated with hypertension compared with other regions of the left atrium.

Hypertension Research advance online publication, 22 December 2016; doi:10.1038/hr.2016.169

Keywords: animal model; cardiac remodeling; cardiomyocyte size; fibrosis; HFpEF

INTRODUCTION

Although there have been significant advances in treatment strategies targeting heart failure (HF) and associated complications, effective therapies for HF with preserved ejection fraction (HFpEF) are still missing.^{1,2} HF is manifested by inadequate ventricular output at physiological filling pressures. Nevertheless, almost half of all clinical HF patients appear to have a preserved left ventricle ejection fraction (LVEF).³ The mechanisms by which hypertension predisposes an individual to HFpEF are not completely understood. It is likely that structural remodeling is one of the key elements that contribute to be trigger and substrate for HF.^{4,5} As a result, there is a need to develop an individualized, targeted and novel therapeutic strategy to prevent the development of structural remodeling in hypertensive patients.

Developing preclinical animal models for HFpEF pharmacological treatment strategies is essential. Previous studies have shown that renal wrapping,⁶ angiotensin II infusion⁷ or pressure overload by aortic banding⁸ could induce HFpEF. However, these models

themselves do not duplicate the clinical diastolic dysfunction. Schwarzl *et al.*⁹ created a porcine model of HFpEF by using a combination of DOCA implantation and Western diet (WD).⁹ However, these animals failed to show an increase in fibrosis, whereas fibrosis is common in patients with HFpEF.^{10,11} Therefore, we reasoned that a higher pressure and longer experimental duration might resemble clinical HFpEF more closely in terms of structural remodeling than other methods previously reported. Therefore, our group created a porcine model of severe hypertension and hyperlipidemia using a combination of DOCA implantation, a WD and angiotensin II infusion. Our study provides a unique opportunity for us to study hypertension-induced cardiac structural remodeling in a clinically relevant large animal model of hypertension heart disease. A large animal model permits the detailed regional histological assessment of hypertension-induced structural remodeling. More importantly, we are the first to evaluate systematically the alterations caused by hypertension-induced cardiac structural remodeling. Our findings may provide

¹Department of Cardiology, The First Affiliated Hospital of Soochow University, Suzhou City, Jiangsu Province, People's Republic of China and ²Department of Cardiology, Suzhou Municipal Hospital Affiliated to Nanjing Medical University, Suzhou City, Jiangsu Province, People's Republic of China

³These authors contributed equally to this work and should be considered co-first authors.

Correspondence: Professor Y-f Zhou, Department of Cardiology, The First Affiliated Hospital of Soochow University, 188 Shizi Road, Suzhou City, Jiangsu Province 215006, People's Republic of China.

E-mail: zhouyafeng@medmail.com.cn

Received 26 May 2016; revised 24 September 2016; accepted 21 October 2016

crucial information for the future development of upstream therapy that targets the mechanism of structural remodeling in HFpEF.

METHODS

This project was approved by the Ethics Committee of Soochow University (Suzhou, China). All animals were handled and maintained according to the guidelines for the Care and Use of Laboratory Animals published by the US National Institutes of Health (8th edition, revised, 2011).

Animal model

Ten adult female swine (30–40 kg, 9–12 months old) underwent general anesthesia with tiletamine and zolazepam (Zoletil 20 mg kg⁻¹, intramuscularly). The animals were then intubated, and anesthesia was maintained with intravenous propofol. An osmotic infusion pump (Tricumed Medizintchnik GmbH, Delhi, India) containing 120 mg angiotensin II (Asp-Arg-Val-Tyr-Ile-His-Pro-Phe acetate salt; Sigma, San Francisco, CA, USA) was implanted via the right internal jugular vein to deliver angiotensin II (0.015 mg h⁻¹). A subcutaneous DOCA pellet (100 mg kg⁻¹, 90-day release depot; Innovative Research of America, Sarasota, FL, USA) was implanted at the dorsal aspect of the neck using sterile surgical technique. The pump was refilled at 5, 9 and 13 weeks. The animals were fed a WD containing high amounts of salt, sugar, cholesterol and fat. The other 10 female swine (30–40 kg, 9–12 months old) in the control group were fed a regular diet. All of the animals in both the hypertension group and the control group were permitted free access to water. All animals were killed by injection of 100 mM potassium at the end of 18 weeks.

Measurement of physiological changes

Systolic blood pressure was noninvasively measured by tail cuff before and after treatment. Standard transthoracic echocardiograms were performed using a commercially available echocardiographic system (Vivid q; GE Vingmed, Horten, Norway). Standard two-dimensional and M-mode echocardiography was performed to measure the left atrial diameters and the left ventricle (LV) end-diastolic wall thickness and diameter. Mitral inflow E wave, isovolumetric relaxation time (IVRT) and deceleration time were measured by pulse-wave Doppler, and tissue Doppler was used to measure medial mitral annular early diastolic velocity (*e'*). Then, *E/e'* and *E/A* were calculated.

The invasive hemodynamic assessment was performed under general anesthesia as discussed above at baseline, 12 weeks and 18 weeks after treatment to assess changes in LV function. A 7-Fr combined catheter micromanometer (Millar Instruments, Houston, TX, USA) was calibrated in isotonic saline and then advanced through femoral artery access to the LV to measure the LVEF, LV $\pm dp/dt$ end-systolic pressure–volume relationship (ESPVR) and end-diastolic pressure–volume relationship (EDPVR). All pressure–volume loop data were collected and averaged over 8 to 10 beats at end expiration from the raw pressure and conductance volume data using commercially available software (Conduct NT, Leycom, The Netherlands).

Biomarker assessments

Enzyme-linked immunosorbent Assay Kits were used to obtain biomarker measurements. Brain natriuretic peptide (BNP) (Phoenix Pharmaceuticals, Burlingame, CA, USA) was measured to assess myocardial stretch. The serum levels of total cholesterol, triglyceride, low-density lipoprotein and high-density lipoprotein were measured using Commercially Available Kits (Roche Diagnostics, Madison, WI, USA). Arterial and venous blood samples were collected at the end of the experiment. All serum lipid level data were only obtained from venous blood samples at 18 weeks. All serum BNP data were obtained from both arterial and venous blood samples at 18 weeks.

Histological studies

The animals were killed by injection of 100 mM potassium. The whole porcine hearts were fixed with 10% formaldehyde for histological study. The left and right atria were each cut into four 7- to 10-mm-thick sections from the atrial appendage, posterior wall, anterior wall and atrial roof, perpendicular to the apical–basal axis. Each section was traced and photographed. The LVs were

Table 1 Systemic characteristic and biomarker data at 18 weeks

	Control (n = 10)	Hypertension (n = 10)
Body weight (kg)	64.3 ± 3.5	78.2 ± 4.1*
Heart rate (b.p.m.)	77.2 ± 5.4	81.3 ± 4.2
Total cholesterol (mg dl ⁻¹)	67.4 ± 3.3	543.5 ± 54.9*
LDL cholesterol (mg dl ⁻¹)	23.5 ± 3.1	352.7 ± 32.8*
HDL cholesterol (mg dl ⁻¹)	35.7 ± 2.3	155.4 ± 23.1*
Triglycerides (mg dl ⁻¹)	28.6 ± 6.8	54.7 ± 13.1*
BNP ^a (pg ml ⁻¹)	54.4 ± 19.8	71.2 ± 11.3
BNP ^b (pg ml ⁻¹)	56.9 ± 14.5	71.2 ± 17.3

Abbreviations: BNP, brain natriuretic peptide; HDL, high-density lipoprotein; LDL, low-density lipoprotein.

Values are means plus/minus s.e. **P* < 0.05 vs. control.

^aBNP value was obtained from venous blood samples.

^bBNP value was obtained from arterial blood samples.

each cut into eight 7- to 10-mm-thick sections from the septal wall, anterior wall, posterior wall and lateral wall, perpendicular to the apical–basal axis. Right ventricles were cut from the anterior wall, posterior wall and lateral wall. Because the ventricular walls were too thick, we divided each ventricular wall into two sections. The anterior wall, posterior wall and lateral wall sections were each divided into the subendocardial section and subepicardial sections. The septal wall was divided into left and right parts. Planimetry of the tracings was performed to measure the degree of fibrosis as a percentage of total collagen. The tissues were embedded in paraffin, sectioned into 5- μ m slices and stained with Masson's trichrome. Morphometric analysis of collagen was performed by AxioVision software (Zeiss GmbH, Oberkochen, Germany). The percent area of fibrosis (% area fibrosis) was calculated as the total area of fibrosis (defined as the amount of collagen deposition stained with aniline blue) divided by the sum of the total tissue area in five random fields on each section. The cardiomyocyte cross-sectional area (CSA) was measured in 25 cells from five random fields in each slide stained with hematoxylin and eosin. The ventricular wall data were represented by the average of two sections from each ventricular wall. Two researchers (S-JS and J-LY) independently evaluated the percent area of fibrosis and cardiomyocyte size. Then, the mean of all data from both researchers was calculated.

Statistical analysis

Student's *t*-test was used for between-group comparisons at a given time point. Two-way analysis of variance repeated measurement was used to analyze blood pressure data, and one-way analysis of variance was used to compare histological data between groups in different walls. If the result of analysis of variance was significant, an unpaired Student's *t*-test was used. All data are presented as the mean \pm s.d. with $\alpha = 0.05$ for significance (version 15; SPSS, Chicago, IL, USA).

RESULTS

Twenty pigs were randomized to the control (*n* = 10) and hypertension groups (*n* = 10) at the beginning. None of them died during this period.

Systemic characteristics and biomarker data

At the end of the experiment, animals in the hypertension group weighed more than the controls did. All of the serum lipid levels were markedly higher in the hypertension group (all *P* < 0.05 vs. controls; Table 1). Nevertheless, there were no significant differences in heart rate and serum BNP (all *P* > 0.05 vs. controls; Table 1). The systolic blood pressure progressively rose from 87 mm Hg (at baseline) to 175 mm Hg (at 12 weeks) and slightly fluctuated at a high level during the next several weeks, even without angiotensin II infusion during the past 2 weeks. All systolic blood pressure data are shown in Figure 1a (all *P* < 0.05 vs. baseline).

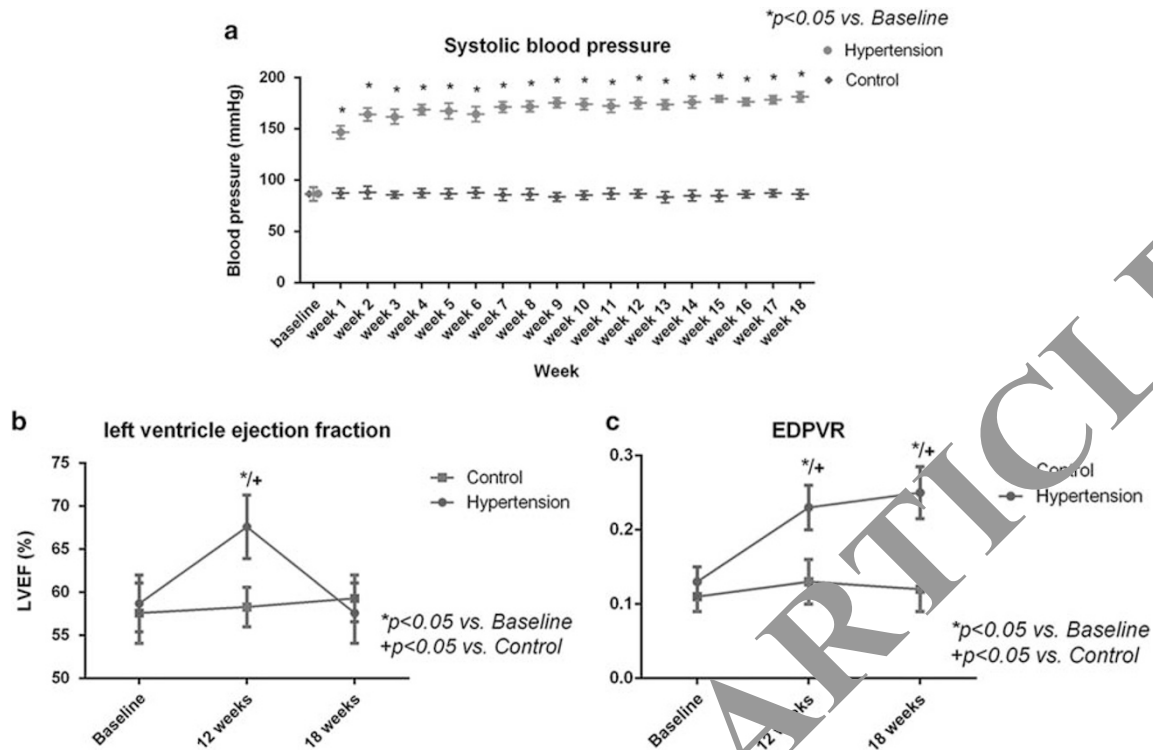


Figure 1 No animals received any treatment at baseline. (a) Systolic blood pressure in the hypertensive group remained higher than in controls after the induction of hypertension. Serial measurements in hypertension group of (b) left ventricle ejection fraction (LVEF) and (c) end-diastolic pressure–volume relationship (EDPVR). A full color version of this figure is available at the *Hypertension Research* journal online.

Table 2 Echocardiographic parameters

	Control (n = 10)			Hypertension (n = 10)		
	Baseline	12 weeks	18 weeks	Baseline	12 weeks	18 weeks
LV septal wall thickness (mm)	11.22±0.54	10.93±0.51	11.17±0.61	11.08±0.54	15.35±0.66 ^{*/+}	17.35±0.63 ^{*/+}
LV posterior wall thickness (mm)	8.92±0.36	8.86±0.52	9.23±0.44	8.78±0.35	15.13±0.44 ^{*/+}	16.51±0.58 ^{*/+}
LV end-diastolic diameter (mm)	47.13±1.02	47.19±1.34	47.31±1.08	48.01±1.40	47.57±1.89	47.23±1.91
LA diameter (mm)	31.42±2.13	30.66±1.91	31.35±2.09	32.22±2.07	35.87±1.66 ^{*/+}	38.96±1.85 ^{*/+}
<i>E/e'</i>	4.07±0.37	5.03±0.41	5.04±0.37	4.92±0.42	5.23±0.40	5.55±0.44 ^{*/+}
<i>E/A</i>	1.07±0.12	1.11±0.09	1.09±0.11	1.10±0.08	0.97±0.12 ^{*/+}	0.92±0.11 ^{*/+}
Deceleration time (ms)	196.66±21.35	196.66±21.32	199.33±18.40	196.41±26.41	223.94±20.42 ^{*/+}	250.86±17.45 ^{*/+}
IVRT (ms)	92.52±17.47	92.59±13.39	100.07±18.40	94.59±12.41	117.54±16.42 ^{*/+}	131.72±13.33 ^{*/+}

Abbreviations: LA, left atrial; LV, left ventricle; IVRT, isovolumetric relaxation time. Values are means plus/minus s.e. **P*<0.05 vs. control. +*P*<0.05 vs. baseline in hypertension group.

Echocardiographic data

Sustained hypertension resulted in thicker end-diastolic septal and posterior walls (*P*<0.05 vs. controls) without any difference in end-diastolic diameter (*P*>0.05 vs. controls). Septal and posterior wall thicknesses at baseline (10.08 and 8.78 mm, respectively) increased up to week 12 (15.35 and 15.13 mm, respectively; all *P*<0.05 vs. baseline) and continued to increase over the next 6 weeks, despite the termination of angiotensin II infusion at the end of 16 weeks. At 18 weeks, both the septal and posterior walls were distinctly thicker than controls (all *P*<0.05 vs. controls). Left atrial diameter was also larger in the hypertension group than in the controls (*P*<0.05 vs. controls). In the hypertension group, *E/e'*, IVRT and deceleration time were significantly increased, whereas *E/A* decreased at 18 weeks (all *P*<0.05 vs. baseline). All of the parameters showed that diastolic

functions of hypertensive pigs were impaired compared with controls (all *P*<0.05 vs. control). All of the echocardiography data are listed in Table 2.

Hemodynamic data

LVEF in the hypertension group experienced a slight increase to 66.3% at 12 weeks (*P*<0.05 vs. baseline) before dipping to 57.6% at 18 weeks (*P*>0.05 vs. baseline; Figure 1b). Although LVEF in the hypertension group was elevated at 12 weeks, there was no significant difference between the groups at 18 weeks (*P*>0.05 vs. controls; Table 3). EDPVR in the hypertension group was higher at 12 and 18 weeks, which reflected increased end-diastolic myocardial stiffness (all *P*<0.05 vs. baseline; Figure 1c). At 18 weeks, EDPVR was also higher in the hypertension group than in the controls (*P*<0.05 vs. controls;

Table 3). ESPVR was similar at baseline, 12 and 18 weeks in the hypertension group ($P > 0.05$ vs. baseline, data not shown). The parameter $+dp/dt$ as a marker of systolic LV function was significantly higher than in controls ($P < 0.05$ vs. controls), whereas $-dp/dt$, as a

marker of LV diastolic function, was significantly lower than in controls ($P < 0.05$ vs. controls). All of the hemodynamic data are listed in Table 3.

Table 3 Invasive hemodynamics data at 18 weeks

	Control (n = 10)	Hypertension (n = 10)
LVEF (%)	58.9 ± 2.3	57.6 ± 3.5
ESPVR	2.24 ± 0.23	2.35 ± 0.18
EDPVR	0.13 ± 0.02	0.25 ± 0.04*
+dp/dt (mm Hg s ⁻¹)	1018 ± 140	1317 ± 123*
-dp/dt (mm Hg s ⁻¹)	-868 ± 113	-946 ± 86*

Abbreviations: ESPVR, end-systolic pressure–volume relationship; EDPVR, end-diastolic pressure–volume relationship; LVEF, left ventricle ejection fraction. Values are means ± s.e. * $P < 0.05$ vs. control.

Histological data

Hematoxylin and eosin staining (Supplementary Figure 1) revealed an increased cardiomyocyte size in all parts of hypertensive hearts compared with non-hypertensive controls (all $P < 0.05$ vs. controls; Figures 2a–d). We also observed a larger CSA of cardiomyocytes in left atria compared with right atria (all $P < 0.05$ vs. right atria, respectively; Figure 2e). However, there were no differences between different walls of the same cavity (all $P > 0.05$, respectively) because the baseline CSA was different between LV and RV, CSA of the hypertension groups was not compared among LV and RV.

The percent area of positive Masson's trichrome staining (Supplementary Figure 2) was also larger in hypertensive animals

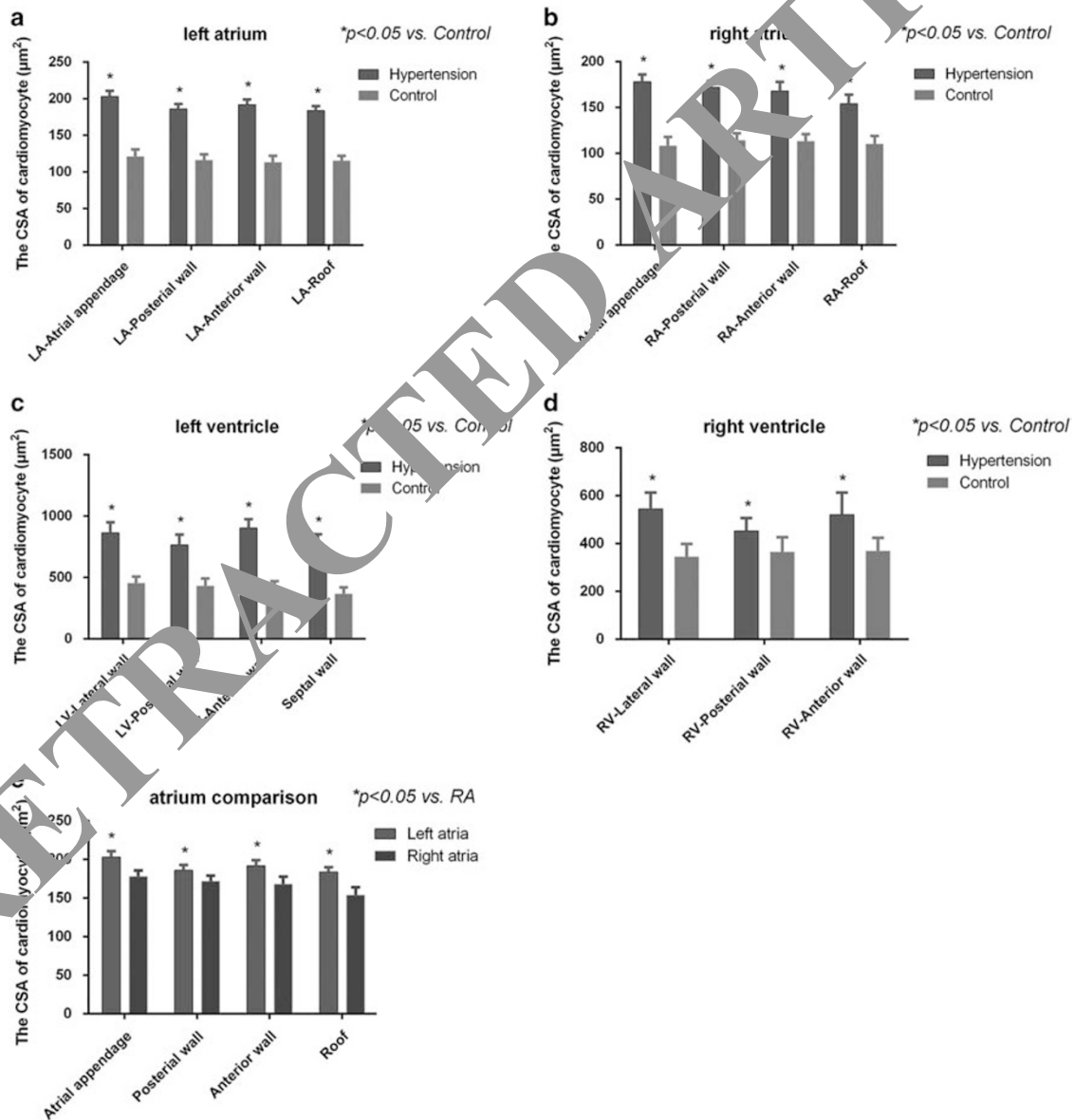


Figure 2 Representative cardiomyocyte cross-sectional area (CSA) of (a) left atrium (hypertension group vs. controls); (b) right atrium (hypertension group vs. controls); (c) left ventricle (hypertension group vs. controls); (d) right ventricle (hypertension group vs. controls); (e) left atrium vs. right atrium in hypertension group. A full color version of this figure is available at the *Hypertension Research* journal online.

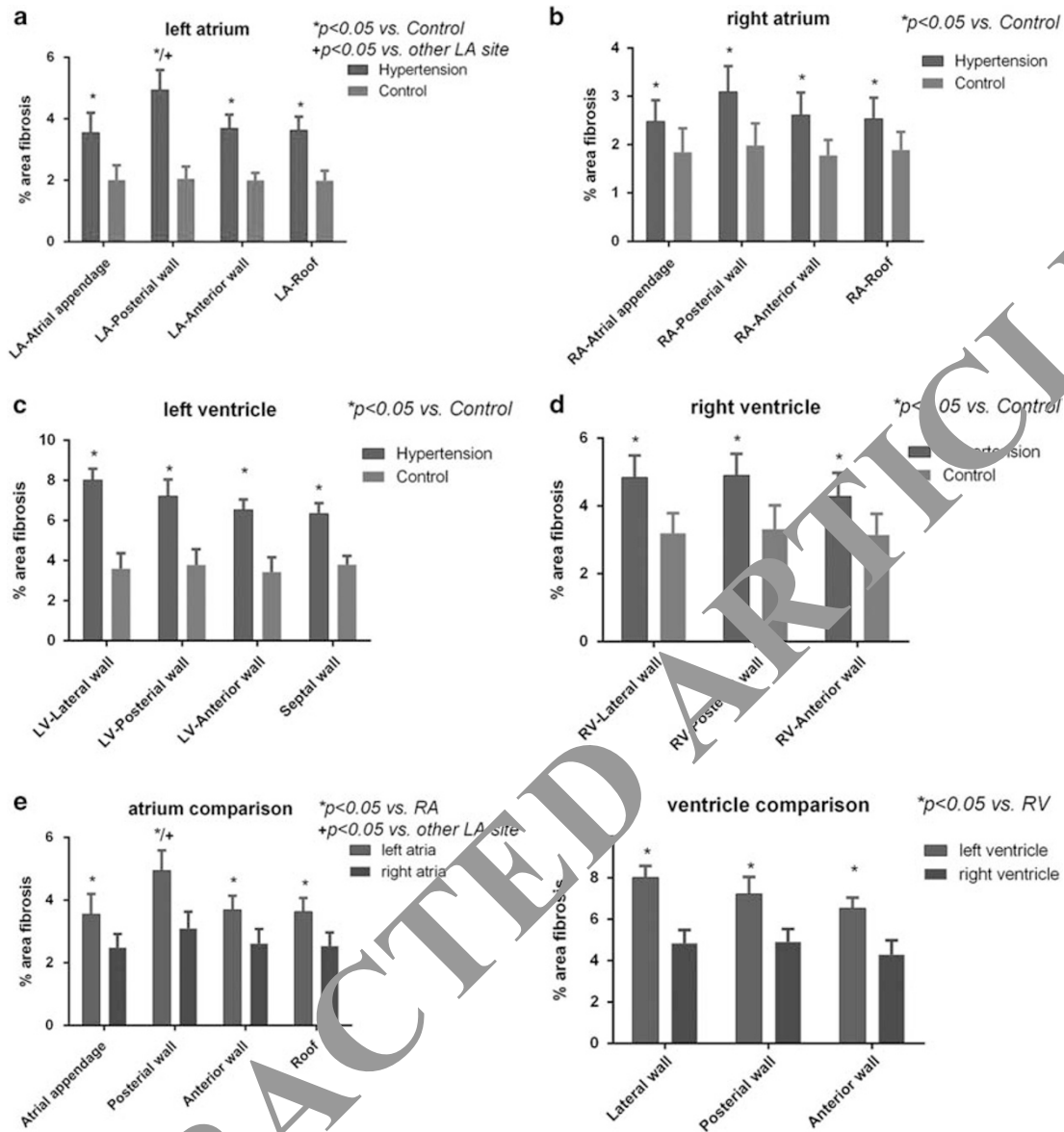


Figure 3 Representative Masson's trichrome staining of (a) left atrium (hypertension group vs. controls); (b) right atrium (hypertension group vs. controls); (c) left ventricle (hypertension group vs. controls); (d) right ventricle (hypertension group vs. controls); (e) left atrium vs. right atrium in hypertension group; (f) left ventricle vs. right ventricle in hypertension group. Fibrosis in the posterior walls of left atria was greater than in other sites of the left atria ($P < 0.05$). There was no other significant difference between different walls of each cavity (all $P > 0.05$). A full color version of this figure is available at the *Hypertension Research* journal online.

(all $P < 0.05$ vs. controls; Figures 3a–d). The positive areas in the left atria and ventricles were also larger compared with the right atria and ventricles (all $P < 0.05$ vs. right atria and right ventricles, respectively; Figures 3e and f). We were surprised to find that different levels of fibrosis were apparent in the left atria of hypertensive animals. The percent area of fibrosis in the posterior walls of hypertensive animals' left atria was larger than other sites of the left atria ($P < 0.05$ vs. other sites in left atria; Figures 3a and e).

DISCUSSION

HFpEF is a significant public health problem worldwide. Recently, studies have revealed that HFpEF is highly associated with hypertension, diabetes, obesity, aging and atrial fibrillation.^{12–14} Therefore,

establishing an animal model is imperative and vital for understanding the mechanisms of and developing therapeutic strategies for HFpEF. Hypertensive response to exercise, which is associated with a higher risk of HF, is more prevalent in hypertensive patients than in normotensive control subjects,¹⁵ whereas metabolic syndrome is an independent risk factor for impaired left atrial function and LV diastolic abnormality.¹⁶ Therefore, we created a porcine model of hypertension and hyperlipidemia using a combination of DOCA implantation, WD and angiotensin II infusion. We only selected female pigs in our experiment, mainly because HFpEF is more likely to affect females than males.¹⁷

Our group successfully established a large animal model of hypertension and hyperlipidemia and then evaluated the structural

remodeling in this model. Although the presence of serum BNP was not increased, concentric remodeling characterized by normal chamber size with higher wall thickness was observed in hypertensive animals. Iwanaga *et al.*¹⁸ reported that thicker walls led to decreased wall stress, which resulted in less elevation in BNP. Furthermore, not all HF patients with preserved ejection fraction showed an increase in BNP.¹⁹

The EDPVR in hypertensive animals were shifted up and to the left compared with that of the normal controls. This was related to the increase in passive chamber stiffness.²⁰ Diastolic function, and data such as E/e' , E/A , IVRT and deceleration time also showed a tendency toward decline according to echocardiographic data. Parameters of LV systolic function, such as LVEF and ESPVR, remained unchanged at 18 weeks, indicating that there was no deficit in LV contractility. Invasive hemodynamic data and echocardiographic data suggested that there was a diastolic dysfunction in hypertensive animals without any significant difference in systolic function. These data may help explain why diastolic dysfunction is common in hypertensive subjects. We found an increase in LVEF in the hypertension group. It is possible that hypertension by angiotensin II promotes hypertrophy, DOCA increases LV preload and the combination of them increases EF temporarily. This animal model presents diastolic dysfunction rather than systolic dysfunction.

We found that fibrosis was developed after angiotensin II infusion, DOCA implantation and WD. Detailed histological analysis showed that although the left atria and ventricles preferred to accumulate stiff fibrosis compared with the right atria and ventricles, there was no significant difference between the different walls of each ventricle. Importantly, fibrosis preferentially developed on the posterior wall of the left atrium compared with other regions of the left atrium and the right atrium, thus signifying a regional difference in susceptibility to atrial remodeling associated with hypertension. Rosita *et al.*²¹ reported that two-thirds of all patients with HFpEF have been or will be afflicted by atrial fibrillation. Extensive interstitial fibrosis was seen in the specimens from animal model of atrial fibrillation, especially in the left atrial posterior wall.²² Our results confirm the observation in the animal model of atrial fibrillation. This finding suggested that our animal model might be clinically relevant for studying the association between HFpEF and atrial fibrillation. Nevertheless, the mechanisms underlying the susceptibility of the posterior wall of the left atrium to remodeling associated with hypertension are still unclear. We also observed that the left atria and ventricles have a larger cardiomyocyte size compared with the right atria and ventricles. These results might suggest that cardiac remodeling associated with hypertension and hyperlipidemia mainly develops in the left part of the heart, although there are also some changes in the right part of the heart. Whether cardiac changes in the right part of the heart contribute to the development of HF is still under exploration.

Limitations

Although we have established an animal model referred to as a model of HFpEF, the E/e' of this model did not match the criteria of HFpEF. The criteria of HFpEF include $E/e' > 15$ or $E/e' > 8$ with $\text{BNP} > 200 \text{ pg ml}^{-1}$, according to the European Society of Cardiology. Furthermore, the serum BNP of this model was not higher than in controls. Whether serum BNP would significantly increase at 24 or even 36 weeks remains unknown. Hypertension and obesity are only two of the many risk factors for HFpEF, which also include older age, kidney disease, anemia and diabetes. It was difficult to assess HF symptoms in the pigs, so whether this model represents stage B or stage C HF is difficult to answer. Because a rapid heartbeat might alter

cardiac fibrosis, we did not increase the heart rate by right atrial pacing to mimic move status. Fibrous tissues commonly occur around vessels, and it is difficult to distinguish fibrous tissue and fibrosis under Masson's trichrome staining. Therefore, we only selected fields without vessels to calculate the percent area of fibrosis. Because we only had histology data at 18 weeks, the time at which structural remodeling began remains unknown. The LVEF decreased from 12 to 18 weeks. Whether it would decrease further than controls at 24 weeks remains unclear.

CONCLUSION

We have established a porcine model of severe hypertension and hyperlipidemia with increased fibrosis, which might provide a more relevant large animal model for the future study of HFpEF. We also found that although cardiac remodeling preferentially occurs in the left atrium and ventricle, there were also some changes in the right part of the heart. Additionally, the posterior wall of the left atrium is more susceptible to atrial remodeling associated with hypertension compared with other regions of the left atrium.

CONFLICT OF INTEREST

The authors declare no conflict of interest.

ACKNOWLEDGEMENTS

This work was supported by grants from National Natural Science Foundation of China (81170174), the Natural Scientific Fund of Jiangsu Province (BK20161226) and Jiangsu Province's Key Provincial Talents Program (20111111). The funders had no roles in study design, data collection and analysis, decision to publish or preparation of the manuscript.

- Schwartzberg S, Redfield MM, From AM, Sorajja P, Nishimura RA, Borlaug BA. Effects of vasodilation in heart failure with preserved or reduced ejection fraction: implications of distinct pathophysiologies on response to therapy. *J Am Coll Cardiol* 2012; **59**: 442–451.
- van Veldhuisen DJ, McMurray JJ. Pharmacological treatment of heart failure with preserved ejection fraction: a glimpse of light at the end of the tunnel? *Eur J Heart Fail* 2013; **15**: 5–8.
- Borlaug BA, Paulus WJ. Heart failure with preserved ejection fraction: pathophysiology, diagnosis, and treatment. *Eur Heart J* 2011; **32**: 670–679.
- Zile MR, Gottdiener JS, Hetzel SJ, McMurray JJ, Komajda M, McKelvie R, Baicu CF, Massie BM, Carson PE. Prevalence and significance of alterations in cardiac structure and function in patients with heart failure and a preserved ejection fraction. *Circulation* 2011; **124**: 2491–2501.
- Shah AM, Shah SJ, Anand IS, Sweitzer NK, O'Meara E, Heitner JF, Sopko G, Li G, Assmann SF, McKinlay SM, Pitt B, Pfeffer MA, Solomon SD. Cardiac structure and function in heart failure with preserved ejection fraction: baseline findings from the echocardiographic study of the Treatment of Preserved Cardiac Function Heart Failure with an Aldosterone Antagonist Trial. *Circ Heart Fail* 2014; **7**: 104–115.
- Munagala VK, Hart CY, Burnett JC Jr, Meyer DM, Redfield MM. Ventricular structure and function in aged dogs with renal hypertension: a model of experimental diastolic heart failure. *Circulation* 2005; **111**: 1128–1135.
- Rienzo M, Bize A, Pongas D, Michineau S, Melka J, Chan HL, Sambin L, Su JB, Dubois-Rande JL, Hittinger L, Berdeaux A, Ghaleh B. Impaired left ventricular function in the presence of preserved ejection in chronic hypertensive conscious pigs. *Basic Res Cardiol* 2012; **107**: 298.
- Marshall KD, Muller BN, Krenz M, Hanft LM, McDonald KS, Dellsperger KC, Emter CA. Heart failure with preserved ejection fraction: chronic low-intensity interval exercise training preserves myocardial O₂ balance and diastolic function. *J Appl Physiol* 2013; **114**: 131–147.
- Schwarzl M, Hamdani N, Seiler S, Alogna A, Manninger M, Reilly S, Zirngast B, Kirsch A, Steendijk P, Verderber J, Zweiker D, Eller P, Höfler G, Schauer S, Eller K, Maechler H, Pieske BM, Linke WA, Casadei B, Post H. A porcine model of hypertensive cardiomyopathy: implications for heart failure with preserved ejection fraction. *Am J Physiol Heart Circ Physiol* 2015; **309**: H1407–H1418.
- van Heerebeek L, Hamdani N, Falcao-Pires I, Leite-Moreira AF, Begieneman MP, Bronzwaer JG, van der Velden J, Stienen GJ, Laarman GJ, Somsen A, Verheugt FW, Niessen HW, Paulus WJ. Low myocardial protein kinase G activity in heart failure with preserved ejection fraction. *Circulation* 2012; **126**: 830–839.
- Westermann D, Lindner D, Kasner M, Zietsch C, Savvatis K, Escher F, von Schlippenbach J, Skurk C, Steendijk P, Riad A, Poller W, Schultheiss HP,

- Tschope C. Cardiac inflammation contributes to changes in the extracellular matrix in patients with heart failure and normal ejection fraction. *Circ Heart Fail* 2011; **4**: 44–52.
- 12 Lam CS, Lyass A, Kraigher-Krainer E, Massaro JM, Lee DS, Ho JE, Levy D, Redfield MM, Pieske BM, Benjamin E, Vasan RS. Cardiac dysfunction and noncardiac dysfunction as precursors of heart failure with reduced and preserved ejection fraction in the community. *Circulation* 2011; **124**: 24–30.
- 13 Ho JE, Lyass A, Lee DS, Vasan RS, Kannel WB, Larson MG, Levy D. Predictors of new-onset heart failure: differences in preserved versus reduced ejection fraction. *Circulation* 2012; **6**: 279–286.
- 14 Kane GC, Karon BL, Mahoney DW, Redfield MM, Roger VL, Burnett JC Jr, Jacobsen SJ, Rodeheffer RJ. Progression of left ventricular diastolic dysfunction and risk of heart failure. *JAMA* 2011; **306**: 856–863.
- 15 Lee SE, Youn JC, Lee HS, Park S, Lee SH, Cho IJ, Shim CY, Hong GR, Choi D, Kang SM. Left atrial volume index is an independent predictor of hypertensive response to exercise in patients with hypertension. *Hypertens Res* 2015; **38**: 137–142.
- 16 Fang NN, Sui DX, Yu JG, Gong HP, Zhong M, Zhang Y, Zhang W. Strain/strain rate imaging of impaired left atrial function in patients with metabolic syndrome. *Hypertens Res* 2015; **38**: 758–764.
- 17 Kawasaki M, Tanaka R, Ono K, Minatoguchi S, Watanabe T, Arai M, Nishigaki K, Noda T, Watanabe S, Minatoguchi S. Impact of gender and healthy aging on pulmonary capillary wedge pressure estimated by the kinetics-tracking index using two-dimensional speckle tracking echocardiography. *Hypertens Res* 2016; **39**: 327–333.
- 18 Iwanaga Y, Nishi I, Furuichi S, Noguchi T, Sase K, Kihara Y, Goto Y, Nonogi H. B-type natriuretic peptide strongly reflects diastolic wall stress in patients with chronic heart failure: comparison between systolic and diastolic heart failure. *J Am Coll Cardiol* 2006; **47**: 742–748.
- 19 Anjan VY, Loftus TM, Burke MA, Akhter N, Fonarow GC, Gheorghiade M, Shah SJ. Prevalence, clinical phenotype, and outcomes associated with normal B-type natriuretic peptide levels in heart failure with preserved ejection fraction. *Am J Cardiol* 2012; **110**: 870–876.
- 20 Dorfs S, Zeh W, Hochholzer W, Jander N, Kienzle R-P, Pieske B, Neumann FJ. Pulmonary capillary wedge pressure during exercise and long-term mortality in patients with suspected heart failure with preserved ejection fraction. *Eur Heart J* 2014; **35**: 3103–3112.
- 21 Zakeri R, Chamberlain AM, Roger VL, Redfield MM. Temporal relationship and prognostic significance of atrial fibrillation in heart failure patients with preserved ejection fraction: a community-based study. *Circulation* 2013; **128**: 1087–1093.
- 22 Tang M, Zhang S, Sun Q, Huang C. Alterations in electrophysiology and tissue structure of the left atrial posterior wall in a canine model of atrial fibrillation caused by chronic atrial dilatation. *Circ J* 2007; **71**: 1636–1642.

Supplementary Information accompanies the paper on Hypertension Research website (<http://www.nature.com/hr>)

RETRACTED ARTICLE